BLACK HOLES

Black hole spin–orbit misalignment in the x-ray binary MAXI J1820+070

Juri Poutanen[1,2,3]*, Alexandra Veledina[1,3,2], Andrei V. Berdyugin[1], Svetlana V. Berdyugina[4], Helen Jermak[5], Peter G. Jonker[6,7], Jari J. E. Kajava[1,8], Ilia A. Kosenkov[1], Vadim Kravtsov[1], Vilppu Piirola[1], Manisha Shrestha[5,9], Manuel A. P. Torres[10,11], Sergey S. Tsygankov[1,2]

The observational signatures of black holes in x-ray binary systems depend on their masses, spins, accretion rate, and the misalignment angle between the black hole spin and the orbital angular momentum. We present optical polarimetric observations of the black hole x-ray binary MAXI J1820+070, from which we constrain the position angle of the binary orbital. Combining this with previous determinations of the relativistic jet orientation, which traces the black hole spin, and the inclination of the orbit, we determine a lower limit of 40° on the spin-orbit misalignment angle. The misalignment must originate from either the binary evolution or black hole formation stages. If other x-ray binaries have similarly large misalignments, these would bias measurements of black hole masses and spins from x-ray observations.

Black holes can be characterized with just two parameters: mass and spin. When a black hole resides in a binary system, accreting material from a companion donor star through the accretion disk, there are additional parameters that determine its observational signatures: the mass accretion rate and the misalignment angle between the black hole spin and the orbital axis. Standard methods to measure black hole spin from x-ray observations—iron line spectroscopy (*1*) or modeling of the accretion disk spectrum (*2*)—assume that the misalignment angle is small. Conversely, the standard interpretation of low-frequency quasi-periodic oscillations in x-ray and optical observations of black hole x-ray binaries as precession of the accretion disk (*3*–*5*) requires the assumption that the misalignment angle is non-negligible. Substantial misalignment is theoretically predicted for x-ray binaries that received high velocities during formation (*6*). The misalignment angle must be inherited from the formation process, because it can only decrease when the black hole is accreting (*7*). Gravitational wave observations of merging black holes have detected signatures of orbital precession (*8*), indicating nonzero misalignment in these systems (*9*), though they might not be representative of the wider population.

Measuring the misalignment angle in x-ray binaries requires determining the three-dimensional orientation of the black hole spin and orbital axis. Accreting black holes often show relativistic jets, which are launched along an axis determined by the black hole spin direction (*10*). The jet inclination angle can be directly obtained in some cases from radio observations (*11*), whereas the jet position angle can be measured using either radio or x-ray imaging. Combining these two angles allows the black hole spin orientation to be determined. Orbital parameters such as period and orbital inclination can be determined using spectroscopic measurements of radial velocities of the donor star taken during quiescence, the stage at which accretion to the black hole is reduced and optical emission is not dominated by the accretion disk, through orbital modulation of the optical photometry and using constraints from the presence or absence of x-ray and optical disk eclipses (*12*).

The black hole x-ray binary MAXI J1820+070 was discovered as a transient x-ray source on 11 March 2018 (*13*). X-ray quasi-periodic oscillations detected shortly after this discovery were observed for >100 days (*14*). Ejections of material traveling at relativistic velocities have been observed from this source in both radio and x-rays, indicating that the jet inclination (measured from the line of sight) is $i_{\rm jet} = 63°\pm3°$ and the position angle (measured on the plane of the sky from north to east) is $\theta_{\rm jet} = 25.^{\circ}1\pm1.^{\circ}4$ (*15*–*17*). Both angles were determined to be stable over the observed duration of the outburst. The orbital inclination has been constrained to the range $66° < i_{\rm orb} < 81°$ by the lack of x-ray eclipses and the detection of grazing optical eclipses (*12*). Determination of the orientation of the orbital axis requires one further parameter, the orbital position angle $\theta_{\rm orb}$.

We monitored MAXI J1820+070 in the optical B, V, and R photometric bands using double image polarimeters (*18*, *19*) during the 2018 outburst and quiescence. We obtained the source intrinsic linear polarization by subtracting the foreground interstellar polarization, measured from nearby field stars. During the outburst, when the relativistic jets were detected at radio frequencies, the intrinsic linear polarization degree (PD) in the V and R bands reached 0.5% at a polarization angle [(PA), also measured from north to east)] of 23° to 24°, which coincides with the jet position angle within the uncertainties (*20*, *21*). After the source faded in the x-rays, the PD increased by a factor of 5 to 10 and the PA changed by 40°±4° to −17°±4° (Fig. 1 and table S1) (*22*). This increase in PD is most prominent in the B band, which also has the highest PD in the range 1.5 to 5%, whereas the R-band polarization changes from 0.4 to 2%. The PA is most precisely determined in the B band, which also shows the least variability, with the mean being $\langle {\rm PA} \rangle = -19.^{\circ}7\pm1.^{\circ}2$.

We identify three properties of the quiescent-state polarization: (i) It is strongest in the blue part of the optical, with approximate dependence on frequency ν as $PD(\nu) \propto \nu^3$ (Fig. 2 and table S1); (ii) the PD remains high in the range 0.5 to 5% and the PA is stable; and (iii) the PA undergoes apparently stochastic variations with an amplitude of <10° with no dependence on the orbital phase (*23*). These properties constrain the mechanism of the polarized emission. We modeled broadband photometric data obtained

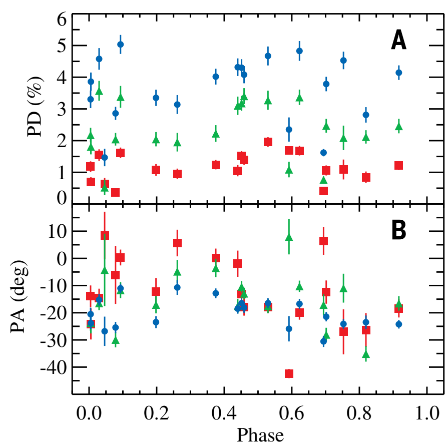

Fig. 1. Observed optical polarization properties of MAXI J1820+070. (**A**) Intrinsic PD and (**B**) PA of MAXI J1820+070 during quiescence are shown as a function of orbital phase (using a published ephemeris) (*23*). The intrinsic values were obtained from the observed ones by subtracting the foreground interstellar polarization, which is measured from nearby field stars. Blue circles, green triangles, and red squares correspond to the B, V, and R bands, respectively, with error bars showing the 68% confidence levels. Polarization is strongest in the B band and weakest in the R band, although the angle does not change substantially.

[1]Department of Physics and Astronomy, FI-20014 University of Turku, Finland. [2]Space Research Institute (IKI) of the Russian Academy of Sciences, 117997 Moscow, Russia. [3]Nordic Institute for Theoretical Physics (Nordita), KTH Royal Institute of Technology and Stockholm University, SE-10691 Stockholm, Sweden. [4]Leibniz-Institut für Sonnenphysik, 79104 Freiburg, Germany. [5]Astrophysics Research Institute, Liverpool John Moores University, L3 5RF Liverpool, UK. [6]Department of Astrophysics, Institute for Mathematics, Astrophysics and Particle Physics (IMAPP), Radboud University, NL-6500 GL Nijmegen, Netherlands. [7]Space Research Organisation of the Netherlands (SRON), Netherlands Institute for Space Research, NL-2333, CA Leiden, Netherlands. [8]Centro de Astrobiología, Villanueva de la Cañada, S-28692 Madrid, Spain. [9]Department of Physics and Astronomy, University of Denver, Denver, CO 80208, USA. [10]Instituto de Astrofísica de Canarias, E-38205 La Laguna, Tenerife, Spain. [11]Departamento de Astrofísica, Universidad de La Laguna, E-38206 La Laguna, Tenerife, Spain.
*Corresponding author. Email: juri.poutanen@utu.fi

with the Liverpool Telescope and the Swift Ultraviolet and Optical Telescope (UVOT) together with the polarized fluxes (Fig. 2). We decomposed the total spectral energy distribution into three components: a companion star (contributing ~25% to the R-band flux) (*24*), an accretion disk with inner temperature $T_{\rm d} \approx 6200$ K and inner radius $R_{\rm d} \approx 6 \times 10^{10}$cm, and an additional ultraviolet (UV) component with blackbody temperature $T_{\rm bb} \approx 15,000$ K and radius $R_{\rm bb} \approx 9 \times 10^9$ cm (table S4). The properties of the polarized flux are consistent with being produced by the UV component with constant PD of 5 to 8%.

The jet cannot be the source of the polarized emission because its optically thin synchrotron spectrum is red, which is inconsistent with the observed blue spectrum of polarized light. Moreover, the PA is offset by ~40° from the jet position angle. The absence of detectable orbital variations in the PA excludes a hot spot origin. An optically thick accretion disk is excluded by the high PD and blue spectrum. A potential source of the polarized emission is scattering of the accretion disk's radiation in the hot, optically thin, geometrically thick accretion flow close to the disk's inner radius (*22*, *25*), which may also be responsible for the observed UV excess. This mechanism would produce polarization parallel to the meridional plane, i.e., the plane formed by the orbital axis and the direction toward the observer. Another possibility is dust scattering, thought to be responsible for the blue polarized spectra observed from accretion disks around some supermassive black holes (*26*). The presence of dust in quiescent-state black hole x-ray binaries has been inferred from the detection of the mid-IR excess in two systems (*27*). If dust is located within a flattened envelope, in the wind around the accretion disk, or in a circumbinary disk, the resulting polarization vector would also be parallel to the meridional plane. However, if dust forms an extended, approximately spherical structure at a high elevation above the accretion disk, the polarization would be perpendicular to the meridional plane. We consider the latter scenario to be implausible, as a nearly spherical envelope cannot produce the high observed PD. A dust scattering mechanism would not explain the UV excess because the disk does not emit in that range and hence there are no photons to be scattered by the dust.

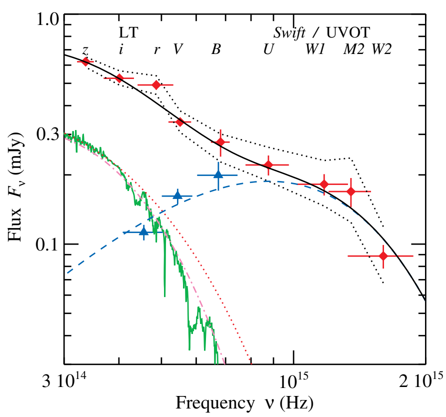

Fig. 2. Spectral energy distribution. The average spectral energy distribution (SED) of MAXI J1820+070 (red diamonds) as observed with the Liverpool Telescope (LT) and Swift UVOT in July 2020 and corrected for reddening, with color excess $E(B-V) = 0.29$. The photometric bands are indicated at the top of the figure. The black dotted lines give the lower and upper limits on the flux for lower and higher extinction with $E(B-V) =$ 0.25 and 0.325, respectively. The polarized flux divided by the best-fitting model polarization degree $P_{\rm UV}$ = 0.055 (i.e., multiplied by a factor of ~18) is indicated by blue triangles. Error bars show 68% confidence levels. The solid black line gives the total model flux consisting of the companion star modeled as a blackbody (pink dot-dashed line), accretion disk (red dotted line), and a hot blackbody (blue dashed line). The spectrum of a K7 star (*24*) is shown for comparison (solid green line).

Independent of the spectral modeling and geometry of the emission, the stability of the PA (most evident in the B band, Fig. 1) over the orbital phase suggests that the polarization is related to the orbital axis, either parallel or perpendicular to it. Hence, the observed PA provides information about the position angle of the orbital axis. The misalignment angle β can be determined from

$$\cos\beta = \cos i_{\rm bh} \cos i_{\rm orb} + \sin i_{\rm bh} \sin i_{\rm orb} \cos\Delta \qquad (1)$$

where $i_{\rm bh}$ is the inclination of the black hole spin vector (measured from the line of sight) and $\Delta = \theta_{\rm bh} - \theta_{\rm orb}$ is the difference between the position angles of the black hole spin vector $\theta_{\rm bh}$ and the orbital angular momentum $\theta_{\rm orb}$ (the geometry is illustrated in Fig. 3). If the black hole spin vector is directed along the southern approaching jet, then its inclination is $i_{\rm bh} = i_{\rm jet} = 63° \pm 3°$ and its position angle is $\theta_{\rm bh} = 180° + \theta_{\rm jet} = 205.^\circ1 \pm 1.^\circ4$ (*15*–*17*). The smallest misalignment, $\beta \approx 42°$, is achieved when the orbital spin is also directed south at $\theta_{\rm orb} = \langle{\rm PA}\rangle + 180° = 160.^\circ3 \pm 1.^\circ2$ (because the PA has an ambiguity of 180°) at the inclination $i_{\rm orb} \approx 73°$. The probability distribution for β in this case is shown in Fig. 4. The radial velocity measurements (*12*) do not differentiate between orbital inclinations $i_{\rm orb}$ and $180° - i_{\rm orb}$ so there is a second solution with $i_{\rm orb} \approx 107°$ and $\beta \approx 63°$. If either the orbital angular momentum or the black hole spin is instead directed to the north, the black hole rotation is then retrograde, resulting in $\beta \approx 117°$ or 138° for the same two solutions for the orbital inclination as above.

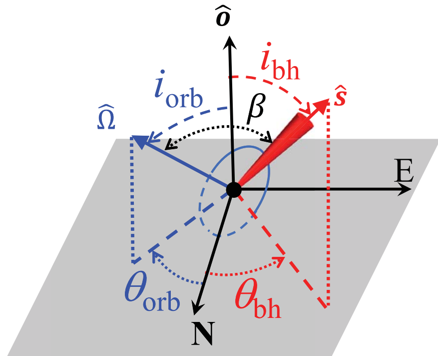

Fig. 3. Geometry of the system from the observer's perspective. The gray plane is the plane of the sky, labelled with north and east axes, perpendicular to the line of sight toward the observer $\hat{o}$. The angles between the line of sight and the vectors of the orbital angular momentum $\hat{\Omega}$ and and the black hole spin $\hat{s}$ are the inclinations $i_{\rm orb}$ and $i_{\rm bh}$. The corresponding position angles $\theta_{\rm orb}$ and $\theta_{\rm bh}$ are the azimuthal angles projected onto the sky, measured from north to east. The misalignment angle β is defined as the angle between $\hat{s}$ and $\hat{\Omega}$. The red cone indicates the jet and the blue ellipse indicates the companion star orbit around the black hole, which is at the coordinate center.

If the polarization vector is perpendicular to the meridional plane, the orbital position angle can take values $\theta_{\rm orb} = \langle{\rm PA}\rangle + 90°$ or $\langle{\rm PA}\rangle + 270°$. This geometrical arrangement leads to nearly identical values for β because the difference between jet position angle and $\langle{\rm PA}\rangle$ is ~45°. All possible cases for the orientations of the black hole and orbital spins, the resulting values for β, and the azimuthal angle of the black hole spin in the orbital plane are listed in table S5. Corresponding probability distributions are shown in figs. S4 and S5.

The difference of ≈45° between the jet position angle and the PA indicates ≳40° misalignment between the black hole spin and the orbital angular momentum. This result is independent of modeling or geometric ambiguities because it relies only on the observed difference between the polarization angle and jet position angle.

During outbursts, when material reaches the black hole, this misalignment affects the innermost regions of the accretion disk. For a nonzero spin, particles moving around the black hole—in orbits tilted with respect to the black hole equatorial plane—undergo precession at a rate that decreases with radius (*3*). Hence, a tilted disk is subject to twist and warp. A high misalignment adds complications to the models of quasi-periodic oscillations observed in black hole x-ray binaries, which rely on precession of the inner parts of the accretion flow, implying that the whole

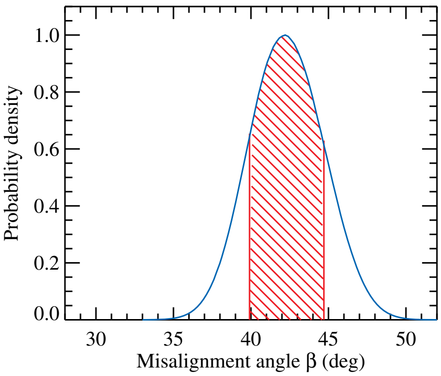

Fig. 4. Probability distribution function for the misalignment angle. The distribution normalized to the peak value is shown for the smallest misalignment angle possible. This case corresponds to the black hole spin directed along the southern approaching jet and the orbital spin being directed south at position angle $\theta_{orb} = \langle PA \rangle + 180°$ and inclination $i_{orb} \approx 73°$. The red hatched region corresponds to the 68% confidence interval (i.e., between 16th and 84th percentiles of the posterior probability distribution). Distributions of β for the other seven possible combinations of θ_{orb}, i_{orb}, and i_{bh} are shown in fig. S4.

flow is misaligned by 2β from the orbital axis in some phases (*3*). For β ~ 40°, the inner parts of the accretion disk would need to become almost perpendicular to its outer parts. Most models assume smaller misalignment angles, typically β ~ 10° to 20° (*3*, *4*, *5*) although highly inclined possibilities with β ~ 45° to 65° have sometimes been considered (*28*).

High misalignment has previously been suggested on the basis of observations of the gamma-ray light curves produced by the jet in Cyg X-3 (*29*), and differences between orbital and jet inclination angles are ~15° in GRO J1655–40 (*7*) and ~50° in V4641 Sgr (*30*) though the latter is highly uncertain. Misalignment has also been theorized on the basis of the inferred high kick velocities of x-ray binaries acquired during formation (*6*). For the black hole x-ray binary MAXI J1820+070, the high misalignment was identified only after obtaining the constraints on the position angle of the orbital angular momentum θ_{orb}. Without information on the binary plane orientation, we would have obtained only a lower limit on the misalignment angle in MAXI J1820+070 of ≳5° because the orbital inclination is only marginally different from the jet inclination.

Our results demonstrate the need to treat the misalignment angle as a free parameter when measuring black hole masses and spins. Assuming that the black hole spin and the orbital angular momentum are aligned introduces a systematic bias on measurements (*12*, *15*, *31*). A large misalignment angle is expected to drive precession of the binary orbital plane, altering the gravitational waves emitted during a subsequent merger event (*9*). Evidence for orbital precession has been found from population properties of black hole mergers observed using gravitational waves (*8*).

REFERENCES AND NOTES

1. C. S. Reynolds, *Space Sci. Rev.* **183**, 277–294 (2014).
2. J. E. McClintock, R. Narayan, J. F. Steiner, *Space Sci. Rev.* **183**, 295–322 (2014).
3. P. C. Fragile, O. M. Blaes, P. Anninos, J. D. Salmonson, *Astrophys. J.* **668**, 417–429 (2007).
4. A. Ingram, C. Done, P. C. Fragile, *Mon. Not. R. Astron. Soc.* **397**, L101–L105 (2009).
5. A. Veledina, J. Poutanen, A. Ingram, *Astrophys. J.* **778**, 165 (2013).
6. P. Atri *et al.*, *Mon. Not. R. Astron. Soc.* **489**, 3116–3134 (2019).
7. T. J. Maccarone, *Mon. Not. R. Astron. Soc.* **336**, 1371–1376 (2002).
8. R. Abbott *et al.*, *Astrophys. J. Lett.* **913**, L7 (2021).
9. T. A. Apostolatos, C. Cutler, G. J. Sussman, K. S. Thorne, *Phys. Rev. D* **49**, 6274–6297 (1994).
10. J. C. McKinney, A. Tchekhovskoy, R. D. Blandford, *Science* **339**, 49–52 (2013).
11. I. F. Mirabel, L. F. Rodríguez, *Annu. Rev. Astron. Astrophys.* **37**, 409–443 (1999).
12. M. A. P. Torres *et al.*, *Astrophys. J. Lett.* **893**, L37 (2020).
13. T. Kawamuro *et al.*, MAXI/GSC detection of a probable new X-ray transient MAXI J1820+070. The Astronomer's Telegram no. 11399 (2018).
14. H. Stiele, A. K. H. Kong, *Astrophys. J.* **889**, 142 (2020).
15. P. Atri *et al.*, *Mon. Not. R. Astron. Soc.* **493**, L81–L86 (2020).
16. J. S. Bright *et al.*, *Nat. Astron.* **4**, 697–703 (2020).
17. M. Espinasse *et al.*, *Astrophys. J. Lett.* **895**, L31 (2020).
18. V. Piirola, A. Berdyugin, S. Berdyugina, "DIPOL-2: a double image high precision polarimeter" in *Proc. SPIE 9147, Ground-based and Airborne Instrumentation for Astronomy V* (Society of Photo-Optical Instrumentation Engineers, 2014), p. 91478I; doi: 10.1117/12.2055923
19. V. Piirola, I. A. Kosenkov, A. V. Berdyugin, S. V. Berdyugina, J. Poutanen, *Astron. J.* **161**, 20 (2021).
20. A. Veledina *et al.*, *Astron. Astrophys.* **623**, A75 (2019).
21. I. A. Kosenkov *et al.*, *Mon. Not. R. Astron. Soc.* **496**, L96–L100 (2020).
22. Materials and methods are available as supplementary materials.
23. M. A. P. Torres *et al.*, *Astrophys. J. Lett.* **882**, L21 (2019).
24. A. J. Pickles, *Publ. Astron. Soc. Pac.* **110**, 863–878 (1998).
25. R. Narayan, J. E. McClintock, I. Yi, *Astrophys. J.* **457**, 821 (1996).
26. W. Webb, M. Malkan, G. Schmidt, C. Impey, *Astrophys. J.* **419**, 494 (1993).
27. M. P. Muno, J. Mauerhan, *Astrophys. J.* **648**, L135–L138 (2006).
28. M. Liska *et al.*, *Mon. Not. R. Astron. Soc.* **507**, 983–990 (2021).
29. A. A. Zdziarski *et al.*, *Mon. Not. R. Astron. Soc.* **479**, 4399–4415 (2018).
30. J. A. Orosz *et al.*, *Astrophys. J.* **555**, 489–503 (2001).
31. X. Zhao *et al.*, *Astrophys. J.* **916**, 108 (2021).
32. A. V. Berdyugin *et al.*, *Zenodo* (2021); doi: 10.5281/zenodo.5767397
33. J. Poutanen, *Zenodo* (2022); doi: 10.5281/zenodo.5837857

ACKNOWLEDGMENTS

We thank K. Belczynski and A. Zdziarski for comments and suggestions. A.V. thanks the International Space Science Institute (ISSI) in Bern, Switzerland, for providing the environment for stimulating discussions. Our findings are based on observations made with the Nordic Optical Telescope (NOT), owned in collaboration by the University of Turku and Aarhus University, and operated jointly by Aarhus University, the University of Turku, and the University of Oslo, representing Denmark, Finland, and Norway, the University of Iceland and Stockholm University at the Observatorio del Roque de los Muchachos, La Palma, Spain, of the Instituto de Astrofisica de Canarias. We thank the NOT staff for their excellent support. DIPol-UF is a joint effort between University of Turku (Finland) and Leibniz Institute for Solar Physics (Germany). The Liverpool Telescope is operated on the island of La Palma by Liverpool John Moores University in the Spanish Observatorio del Roque de los Muchachos of the Instituto de Astrofisica de Canarias with financial support from the UK Science and Technology Facilities Council. **Funding:** A.V. acknowledges support from the Academy of Finland grant 309308. J.P., A.V., V.K., and S.S.T. received funding from Russian Science Foundation grant 20-12-00364. I.A.K. and V.K. thank the Magnus Ehrnrooth Foundation for support. S.V.B. acknowledges support from ERC Advanced Grant HotMol ERC-2011-AdG-291659. M.A.P.T. acknowledges support from the State Research Agency (AEI) of the Spanish Ministry of Science, Innovation and Universities (MCIU) and the European Regional Development Fund (FEDER) under grant AYA2017-83216-P and a Ramón y Cajal Fellowship (RYC-2015-17854). **Author contributions:** J.P. and A.V. initiated the project, performed modeling, and led writing of the text. A.V.B., V.P., and I.A.K. planned and performed the polarimetric observations. H.J., M.S., and M.A.P.T. planned and executed observations using the Liverpool Telescope and V.K. reduced the photometric data. J.J.E.K. obtained the Swift observations and analyzed the data together with S.S.T., P.G.J., and S.V.B. contributed to the interpretation of the results. All authors provided input and comments on the manuscript. **Competing interests:** We declare no competing interests. **Data and materials availability:** The raw DIPol-UF data are available at Zenodo (*32*). The Liverpool Telescope data are available from https://telescope.livjm.ac.uk/DataProd/ under proposal ID JQ20A01. The Swift data are available at https://heasarc.gsfc.nasa.gov/cgi-bin/W3Browse/swift.pl under Observation IDs 000106272**, with ** being 19 to 22 and 24 to 26. Our software for computing the probability distribution of the misalignment angle and for modelling polarization properties of the hot accretion flow is available at Zenodo (*33*). The parameters of our SED model are listed in table S4 and our derived geometrical parameters are in table S5.

SUPPLEMENTARY MATERIALS

science.org/doi/10.1126/science.abl4679
Materials and Methods
Figs. S1 to S5
Tables S1 to S5
References (*34*–*74*)

15 July 2021; accepted 21 January 2022
10.1126/science.abl4679

Science

Black hole spin–orbit misalignment in the x-ray binary MAXI J1820+070

Juri PoutanenAlexandra VeledinaAndrei V. BerdyuginSvetlana V. BerdyuginaHelen JermakPeter G. JonkerJari J. E. KajavaIlia A. KosenkovVadim KravtsovVilppu PiirolaManisha ShresthaManuel A. P. TorresSergey S. Tsygankov

Science, 375 (6583), • DOI: 10.1126/science.abl4679

Misaligned spin in an x-ray binary
If a black hole is in a close enough binary system with a star, it rips material off the companion. As that material falls into the black hole, it forms an accretion disk that is hot enough to emit optical and x-ray radiation. Poutanen *et al*. used optical polarimetry to determine the orbital axis of a black hole x-ray binary (see the Perspective by Patat and Mapelli). Combining these observations with previous measurements of the black hole spin showed that the two are misaligned by at least 40 degrees. This high misalignment must have been generated during the formation of the black hole, because accretion always brings the two axes closer together. —KTS